Trans-Hydrogen-Bond Scalar Couplings as a Source of Structural Constraints in NMR of Proteins: DFT Analysis

by **Tim Heinz**, **Osvaldo Moreira**, and **Konstantin Pervushin***

Laboratorium für Physikalische Chemie, Swiss Federal Institute of Technology, ETH-Hönggerberg, CH-8093 Zürich
(phone: +41-1-632-0922; fax: +41-1-632-1021)

Dedicated to Professor *Dieter Seebach* on the occasion of his 65th birthday

The conformational dependences of $^{15}N,^{15}N$ and $^{1}H,^{15}N$ *trans*-H-bond spin-spin scalar couplings, $^{h2}J(N,N)$ and $^{h1}J(N,H)$, have been investigated by sum-over-states density-functional-perturbation theory. The distance and angular dependence of the $^{h2}J(N,N)$ and $^{h1}J(N,H)$ coupling constants in the H-bonded arrangement between acetylethylamine and imidazole molecules were examined for a wide range of mutual orientations. These molecules were used to model a structurally important H-bond between the amide backbone of Arg7 and the remote imidazole side chain of His106 in the 44 kDa trimeric enzyme chorismate mutase from *Bacillus subtilis*. The magnitude of $^{h1}J(N,H)$ is relatively insensitive to the sampled rotations around three orthogonal axes centered on the tertiary N-atom of the imidazole, whereas values of $^{h2}J(N,N)$ demonstrated a strong dependence on the value of the cone angle θ aligned with the amide group involved in the H-bond. Simple functional approximations have been generated, enabling back calculations of the N···N distance and angle θ of the H-bond, provided that the experimental values of both $^{h2}J(N,N)$ and $^{h1}J(N,H)$ coupling constants are available.

Introduction. – Ever since the discovery of the trans-H-bond $^{h2}J(N,N)$ and $^{h1}J(N,H)$ coupling constants in nucleic acids [1][2], a number of NMR techniques have been developed to measure values of these couplings with high precision [3] and to correlate nuclear spins across H-bonds. In contrast to earlier experimental observables [4][5], these couplings can be used to identify all partners of the H-bond – the donor, the proton, and the acceptor atoms – in an NMR experiment. This novel spectroscopic means was applied to structural, dynamic, and physicochemical studies of a variety of DNA, RNA, and protein systems and their complexes [6]. Since most of these couplings included secondary structure, defining backbone-to-backbone or base-to-base interactions, the mere detection of the H-bond partners was frequently enough to sufficiently constrain or confirm the geometries of molecules [1][7]. The development of NMR experiments for the direct detection of backbone-to-side-chain [8][9] or side-chain-to-side-chain [10] H-bonds in proteins promises to increase the precision of NMR structure determination provided that the values of the trans-H-bond couplings as a function of geometrical parameters are known.

In the past, the origin of this binding type has mostly been attributed to electrostatic interactions between the donor and acceptor groups that form the H-bond [4]. Recent NMR experiments [1][2][7][11], quantum-mechanical *ab initio* calculations [12], and X-ray *Compton* scattering experiments [13] unequivocally demonstrated the partially covalent character of some H-bonds, thus explaining their strength and directionality. The H-bonds are found to be directional and are, therefore, suited to play a role in molecular-recognition phenomena [14]. These characteristics can be probed in detail

by *ab initio* computational approaches that employ the finite-perturbation theory (FPT) and the density-functional theory (DFT) [15][16][17]. An analysis of conformational dependencies of a set of trans-H-bond couplings *via* a systematic search through the available conformational space of a given H-bond should provide valuable nonempirical geometric constraints for the 3D-structure reconstruction and optimization based on distance geometry or molecular-dynamics approaches [18][19].

Here, we report the use of quantum-chemical DFT calculations to investigate conformational dependencies of scalar couplings across an H-bond between a backbone amide and a His imidazole group found in the 44 kDa chorismate mutase from *Bacillus subtilis* (BsCM) [9]. This water-soluble enzyme catalyzes the rearrangement of chorismate to prephenate, a key step in the biosynthesis of the amino acids Tyr and Phe [20]. NMR Investigations have revealed a structurally important H-bond at the active site of BsCM between Arg7 and His106. Transverse-relaxation-optimized spectroscopy (TROSY) [21] was exploited to measure the $^{15}N,^{15}N$ and $^{1}H,^{15}N$ *trans*-H-bond scalar couplings, $^{h2}J(N,N)$ and $^{h1}J(N,H)$. Although this H-bond was not identified in the crystal structures of the free enzyme or its complexes with various ligands [20][22], it can be formed by a 180° rotation of His106 around its χ_2 angle [9]. This H-bond is used as a model system to test the applicability of DFT calculations to generate structural constraints based on the values of the experimental trans-H-bond coupling constants and the computed *ab initio* conformational energy.

Computational Methods. – *Orientationally Averaged Scalar Coupling Constants.* The quantum-chemical calculations of the scalar *J*-coupling constants were performed with sum-over-states (SOS-DFPT) [23][24][25]. By definition [26][27], the nuclear spin-spin-coupling tensor $\boldsymbol{J}$ is the second derivative of the total energy ε of the system with respect to the spins *I* of the nuclei M and N,

$$J(\mathrm{M},\mathrm{N})_{uv} = \frac{\partial^2}{\partial I_{\mathrm{M},u}\partial I_{\mathrm{N},v}}\varepsilon\left(I_{\mathrm{M},u}, I_{\mathrm{N},v}\right)\Big|_{I_{\mathrm{M},u}=I_{\mathrm{N},v}=0} \tag{1}$$

where *u* and *v* are the corresponding coordinates *x*, *y*, or *z*. *Eqn. 2* relates the nuclear spin-spin coupling tensor $\boldsymbol{J}$ to the reduced coupling tensor $\boldsymbol{K}$.

$$\boldsymbol{J} = \frac{\hbar}{2\pi}\gamma_{\mathrm{M}}\gamma_{\mathrm{N}}\boldsymbol{K} \tag{2}$$

The reduced coupling tensor $\boldsymbol{K}$ is independent of the magnetogyric ratios γ_{M} and γ_{N} (which could be positive or negative) coming from the electronic structure of the system only. The orientationally averaged value of the nuclear spin-spin coupling tensor $\boldsymbol{J}$ corresponding to the NMR-observable nuclear spin-spin coupling constant $J(\mathrm{M},\mathrm{N})$ is obtained according to *Eqn. 3:*

$$J(\mathrm{M},\mathrm{N}) = \frac{1}{3}\left(J(\mathrm{M},\mathrm{N})_{xx}+J(\mathrm{M},\mathrm{N})_{yy}+J(\mathrm{M},\mathrm{N})_{zz}\right) \tag{3}$$

As usual for nonrelativistic calculations of the $J(\mathrm{M},\mathrm{N})$ coupling constant, only three major contributions to the total Hamiltonian are considered: the *Fermi*-contact (FC), the paramagnetic spin-orbit (PSO), and the diamagnetic spin-orbit (DSO) terms.

DFT Calculations. DFT Calculations were performed with the deMon program [28]. The function basis used for the calculations is IGLO-III [29] except for N-atoms, where the 'substitute' option with the parameter basis (5, 2; 5, 2) was evoked. The exchange-correlation potential was Perdew-86 [30]. To obtain a relatively good accuracy for the coupling constants, the options for the numerical integration were set to 'radial 64' for the enlarged grid and to 'grid fine random' for the regular grids with the perturbation set on N(1) of the imidazole ring. An individual molecular configuration was computed in about 6 h on a 1.8 GHz *Pentium 4* personal computer equipped with the 'fast Rambus' memory.

Model Construction. – The input structure for DFT calculations was prepared by cutting a subset of atoms at C–C bonds from the X-ray structure corrected for the His106 · Arg7 H-bond [9]. Thus, two molecules, acetylethylamine (AEM) and imidazole (IM) in the neutral tautomeric form, in which N(4) bears a proton, were used as input to model the protein backbone around Arg7 and the side chain of His106, respectively (*Fig. 1*). This choice enabled sampling of a large number of conformations simultanuously, minimizing conformational clash on the displacements and rotations studied. The thus-constructed initial molecular configuration was geometrically optimized with the program Gaussian98 at the HF/STO-3G level [31]. Five pseudo-atoms were introduced to define three axes of rotation, ϕ_x, ϕ_y, and ϕ_z, which are shown in *Fig. 1* together with the directions of the positive rotation. The distance displacements along the H-bond were performed with the program Molden [32]. For each subsequently sampled molecular configuration, the energies were calculated by application of DFT with the *Perdew* and *Wang* exchange and correlational functions PW91 [36] and the 6-311G** basis set. These functionals are well-suited to evaluate interactions in *Van der Waals* and H-bonded systems [37]. The binding energies were

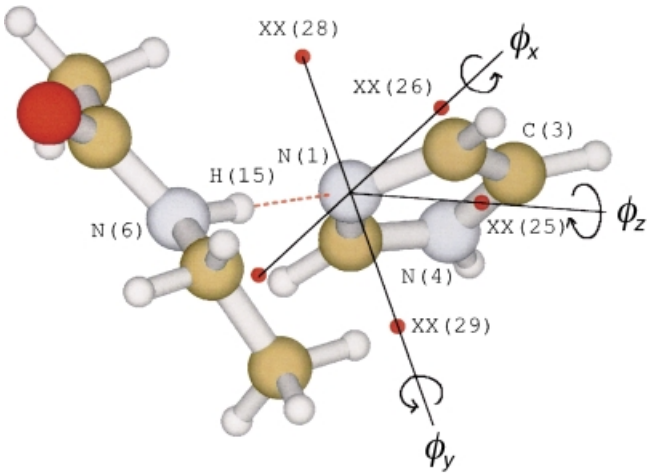

Fig. 1. *Geometry and numbering system of H-bonded AEM and IM molecules.* Pseudo-atoms XX(25), XX(26), XX(27), XX(28) and XX(29) are added to apply ϕ_x, ϕ_y, and ϕ_z rotations to the IM ring. The system represented is in the initial molecular configuration corresponding to the positions of the IM ring found in the X-ray structure of BsCM [22], corrected for the His106 · Arg7 H-bond [9] with ϕ_x, ϕ_y, and ϕ_z set to 0°.

calculated as $\varepsilon_b = \varepsilon(\text{AEM}\cdot\text{IM}) - \varepsilon(\text{AEM}) - \varepsilon(\text{IM})$, and the basis-set superposition error [38] was assessed in terms of a counterpoise correction, although only relative energies are of interest within this context. The reported energies correspond to the optimized geometries. For each molecular configuration generated and optimized, the values of ^{h2}J(N,N) and ^{h1}J(N,H) together with the corresponding FC, PSO, and DSO terms were evaluated with the programs deMon (Version 1) and MASTER (Version 3). An analysis of contributions of the individual molecular orbitals to the FC part of the trans-H-bond scalar couplings [12] was performed with the program deMon. The selected MOs were visualized with the program Molden.

Results and Discussion. – The starting molecular configuration of H-bonded AEM · IM used for the DFT calculations was constructed based on the 1.3 Å resolution X-ray structure of BsCM [22] (see *Computational Methods*). Comparison with the previous DFT calculations of somewhat larger fragments used to model the H-bond between the amide backbone of Arg7 and the remote imidazole side chain of His106 [9] showed that the removal of the Et moiety from the imidazole ring and the truncation of the alanyl dipeptide acetyl-alanyl-*N*-methylamide (Ace-Ala-NMe), used as a standard backbone model in previous studies [9][33], results in a less than 0.5 Hz systematic shift in the values of the trans-H-bond scalar couplings, ^{h2}J(N,N) and ^{h1}J(N,H). To probe different orientations of IM relative to AEM, five pseudo-atoms (XX) were introduced in addition to the structural atoms to define the three orthogonal axes of rotation ϕ_x, ϕ_y, and ϕ_z. *Fig. 1* shows the position and sense of rotation of each of the three selected axes. The *z*-axis connects N(1) to XX(25) atoms and is positioned in the plane of the IM ring. The *y*-axis connects N(1) to X(29) atoms and the *x*-axis connects N(1) to XX(26) atoms, so that XX(26) and XX(27) atoms are in the IM ring plane, and XX(28) and XX(29) atoms are orthogonal to the plane. It should be noted that, in the initial molecular configuration, the vector between the H-bonded N(6) and N(1) atoms deviates from the IM ring-plane by about 10°, preventing the use of the N(1) → N(6) vector as the *z*-axis. When the angles N(6)–N(1)–XX(29) and N(6)–N(1)–XX(27) are set to 90°, the H-bond direction and the *z*-axis coincide. In the initial structure, those angles are found to be 79.9° and 86.4°, respectively. In the optimized structure, H(15) (see *Fig. 1*) is at the distance of 1.035 Å from the covalently bound N(6) and 1.872 Å from the imidazole N(1), resulting in a H-bond length of 2.91 Å and an H-bond angle of 179°. Two additional orthogonal rotations of IM relative to AEM, ψ_x and ψ_y, were introduced with the H(15) atom at the pivotal point. Although both of the ψ_x and ψ_y rotations away from the equilibrium configuration resulted in the decrease of ε_b, they did not affect values of the calculated coupling constants ^{h2}J(N,N) and ^{h1}J(N,H) within the assumed precision of calculations. Thus, additional experimental measurements are required to define the angle N(6)–H(15)–N(1).

Fig. 2 shows the ^{h2}J(N,N) coupling constant as a function of both rotation around the *x*- and *y*-axes, ϕ_x and ϕ_y, and the change in total energy of the system. As expected from the symmetry of the H-bond, the rotation around the *z*-axis does not exert any significant effect on the values of the trans-H-bond couplings and the total energy, and, therefore, was excluded from further analysis. Very similar dependencies of the values of ^{h2}J(N,N) are found for the two orthogonal rotations ϕ_x and ϕ_y (*Figs. 2, b* and *c*). This observation suggests that ^{h2}J(N,N) can be described by a single angular parameter θ,

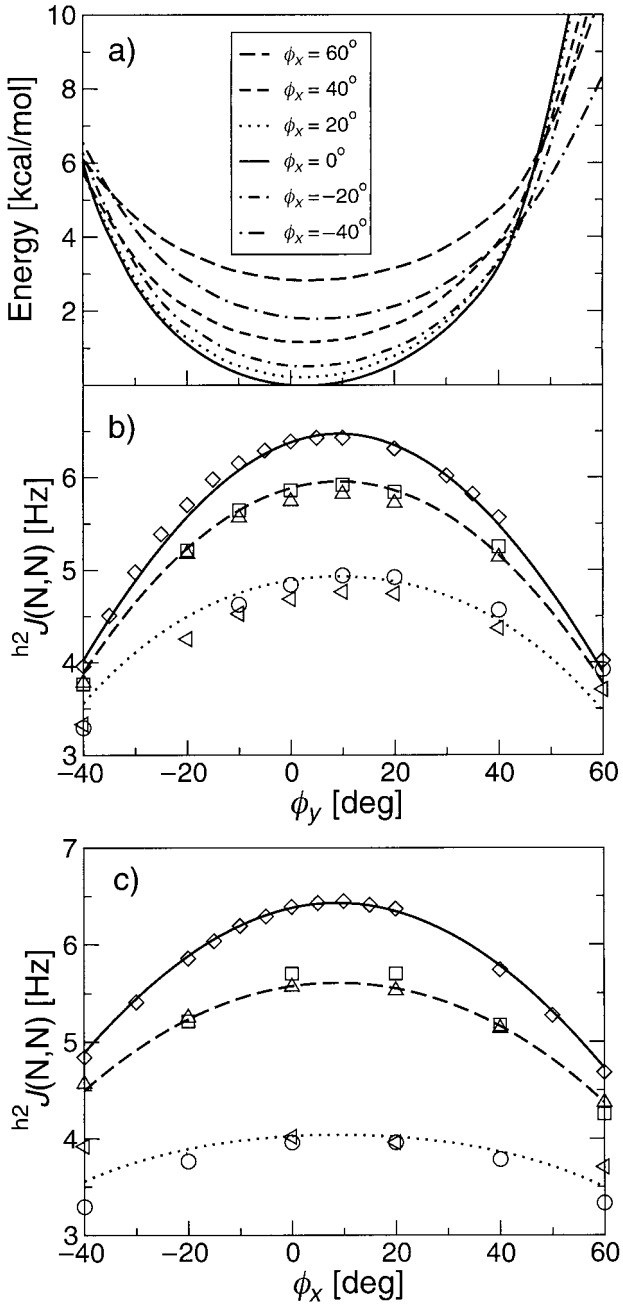

Fig. 2. a) *The total energy of the system;* b) *and* c) *the calculated values of* ^{h2}J*(N,N)* vs. *rotations about the* x- *and* y-*axis, respectively.* In *a*), the energy profiles are given by spliced curves. In *b*) and *c*), the curves represent the approximation given by *Eqn. 5* for $\phi_{x,y} = 0°$ (solid curve), $\phi_{x,y} = -20°$ (dashed line) and $\phi_{x,y} = 40°$ (dotted line). The following symbols indicate the effect of the rotations: $\phi_{x,y} = -40°$ (circles), $\phi_{x,y} = -20$ (squares), $\phi_{x,y} = 0°$ (diamonds), $\phi_{x,y} = 40°$ (triangle, point up), and $\phi_{x,y} = 60°$ (triangle, point left).

which represents a cone angle centered around the N(6) → H(15) vector, as given by *Eqn. 4:*

$$\theta = \arctan\{[\tan^2(a(\phi_x - 8.7^\circ)) + \tan^2(b(\phi_y - 9.3^\circ))]^{1/2}\} \quad (4)$$

where the parameters a and b take the values 0.84 and 1.05, respectively. The offsets of 8.7° and 9.3° in ϕ_x and ϕ_y have no structural significance and only reflect the choice of the initial molecular configuration. In contrast to ^{h2}J(N,N), ^{h1}J(N,H) is practically insensitive to both ϕ_x and ϕ_y rotations (*Fig. 3, a* and *b*). Similar observations were made for the linearly arranged H-bond in the anion $[C{\equiv}^{15}N\cdots H\cdots{}^{15}N{\equiv}C]^-$ [12]. These weak dependencies can be partially attributed to significant contributions of the PSO and DSO terms to the net value of ^{h1}J(N,H) in addition to the main contribution of the FC term. *Fig. 3* shows that the PSO + DSO terms tend to counteract the main contribution of the FC term to ^{h1}J(N,H) at the flanking regions of the ^{h1}J(N,N) (ϕ_x, ϕ_y) curves, thus reducing the dependence of this coupling constant on the angular variables.

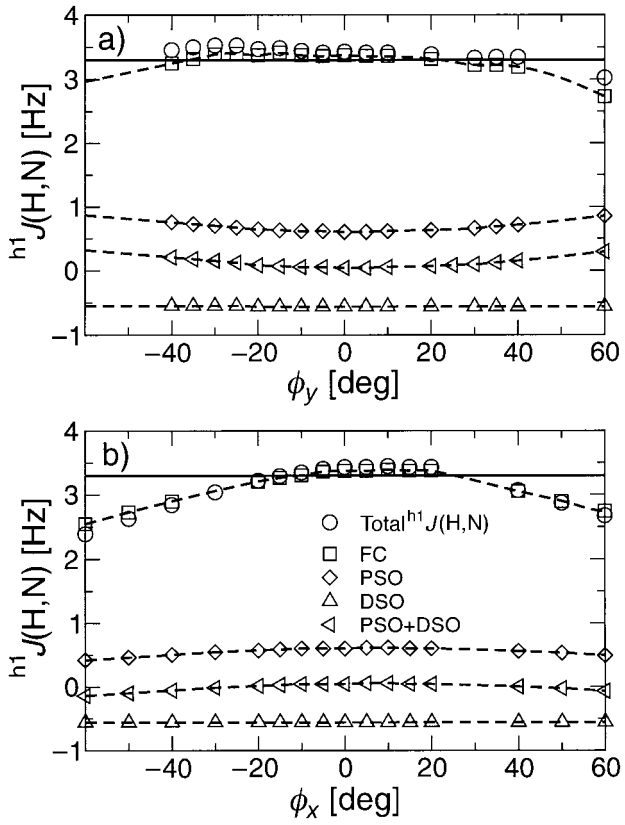

Fig. 3. *The calculated values of ^{h1}J(N,H)* vs. *rotations around the* x- *and* y-*axis.* The individual contributions (FC, PSO, and DSO) to the total ^{h1}J(N,N) coupling constant are displayed and connected by spliced dashed curves. The solid curves represent the approximation given by *Eqn. 6*.

The corresponding contributions of the PSO and DSO terms to the ^{h2}J(N,N) coupling constant are negligible (data not shown).

As is typical for other types of H-bonds [7], both ^{h2}J(N,N) and ^{h1}J(N,H) are strongly sensitive to the distance between donated H-atom and the accepting N-atom, as shown in *Fig. 4*. A sufficiently good fit of the ^{h2}J(N,N) and ^{h1}J(N,H) values can be obtained by means of the r^{-3} polynomial in contrast to the previously proposed exponential dependence [34]. A similar distance dependence was found for the values of the ^{2}H quadrupolar coupling constants (QCC) derived from the NMR data [35], which are defined largely by the electron density at the position of the nucleus. In particular for the protein backbone N–H···O=C H-bond, a correlation to the H-bond length r and the H-bond angle θ was established as QCC(^{2}H)/kHz = 228 + 130 cos(θ)r^{-3}. It should be noted that the total calculated energy has a rather shallow profile around the equilibrium H-bond distance of 2.9 Å, which makes it difficult to rely exclusively on the total energy to sufficiently constrain the H-bond.

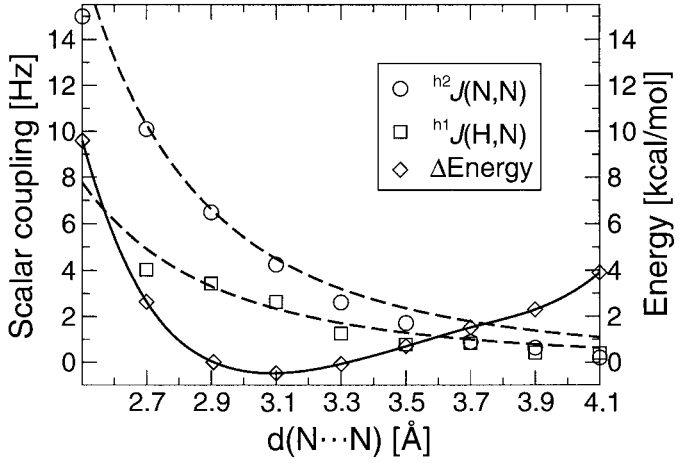

Fig. 4. *Calculated ^{h2}J(N,N) and ^{h1}J(N,H) coupling constants* (left ordinate) *and the total energy* (right ordinate) *as a function of the distance between N(1) and N(6) across the H-bond.* The energy profile is represented by a spliced solid curve. The dashed curves represent the approximation given by *Eqns. 5* and *6*.

All calculated angular and distance dependencies of the ^{h2}J(N,N) and ^{h1}J(N,H) coupling constants can be sufficiently well represented by the functions given in *Eqns. 5* and *6*.

$$^{h2}J(\mathrm{N,N})/\mathrm{Hz} = 20.6{*}\cos(\theta/(r-1.44)^3 \quad (5)$$

$$^{h1}J(\mathrm{N,H})/\mathrm{Hz} = 12.6/(r-1.28)^3 \quad (6)$$

where $\theta = 0^\circ$ defined in *Eqn. 4*.

With $\theta = 0^\circ$, the donated H-atom is located on the line connecting the two N-atoms involved in the H-bond. The calculated values of ^{h2}J(N,N) and ^{h1}J(N,H), approximated by the functional dependencies of *Eqns. 5* and *6* are shown in *Figs. 2–4*. Within the margin of error, ^{h1}J(N,H) does not depend on the H-bond angle θ, in contrast to the

values of $^{h2}J(N,N)$. When both $^{h2}J(N,N)$ and $^{h1}J(N,H)$ are experimentally available, *Eqns. 5* and *6* may be solved for the H-bond distance r and the cone angle θ.

The validity of the approximations in *Eqns. 5* and *6* can be tested with experimentally observed coupling constants in BsCM. For the orientation of the imidazole group found in the corrected X-ray structure (see *Computational Methods*), good agreement between experimental values ($^{h2}J(N,N) = 6.5 \pm 0.2$ Hz and $^{h1}J(N,H) = 2.87 \pm 0.15$ Hz) and calculated values ($^{h2}J(N,N) = 6.8$ Hz and $^{h1}J(N,H) = 2.5$ Hz) of both couplings is obtained [9]. Based on the DFT calculations, we can conclude that the orientation of the imidazole ring found in the corrected structure of BsCM is compatible with the experimental values of $^{h2}J(N,N)$ and $^{h1}J(N,H)$, and no further refinement is needed.

The molecular-orbital analysis performed with the program deMon indicates that, of 42 occupied orbitals, 11 core MOs do not contribute to the trans-H-bond couplings. The individual contributions of higher-lying MOs can be unrealistically large, but cancel each other to a large extent. This assumption significantly complicates the detailed quantitative analysis of contributions of the individual orbitals to the FC component of the scalar couplings, since pairs of groups of MOs with the mutually cancelling contributions to the trans-H-bond couplings should be considered [12]. *Fig. 5* shows MO12, MO14, and MO15, which are responsible (among others) for the transmission of the $^{h2}J(N,N)$ coupling. Despite the difficulties of the quantitative analysis, we can conclude that the MOs with the most-significant contributions to the scalar coupling possess σ symmetry (MO14 and MO15) and exhibit non-negligible coefficients of atoms from both sides of the H-bond. The significant total electron density in the H-bond region between AEM and IM molecules (*Fig. 5, d*) emphasizes the covalent character of the H-bond, although this density does not guarantee the presence of NMR-detectable scalar couplings.

In summary, this paper describes a simple approach to constrain the position of the IM ring on the surface of a cone centered around the H-bonded N/H moiety at a specific distance from the donor group. The method presented relies on the experimental values of $^{h2}J(N,N)$ and $^{h1}J(N,H)$ to calculate the H-bond distance r and the cone angle θ. A further possible conformational restraint, the total energy of the system, is not sufficient to define the geometry of the H-bond, since it exhibits rather shallow dependencies on the angular and distance parameters. The analysis of various contributions to the $^{h2}J(N,N)$ couplings indicates the predominant importance of the FC term, which is not the case for the $^{h1}J(N,H)$ couplings. This might, to some extent, explain different sensitivities of $^{h1}J(N,H)$ and $^{h2}J(N,N)$ to rotations centered on the tertiary N-atom of the H-bond.

Simple functional approximations have been generated that enable back calculation of the N···N distance and angle θ of the H-bond provided that the experimental values of both $^{h2}J(N,N)$ and $^{h1}J(N,H)$ are available. These simple functional dependencies can be easily implemented as conformational constraints in the process of molecular-structure reconstructions based on NMR or even empirical data.

Financial support was obtained from an ETH Zürich internal grant to *K. P.* We thank Drs. *Alessandro Bagno* and *Giacomo Saielli*, University of Padova, Italy, for their help and fruitful discussion on deMon NMR setup, *Alexander Maltsev* and *Tomas Skalicky*, University of Fribourg, Switzerland, for their helpful suggestions on Gaussian98, Dr. *Serguei Patchkovskii*, Steaci Institute for Molecular Science, Ottawa, Canada, for his help in

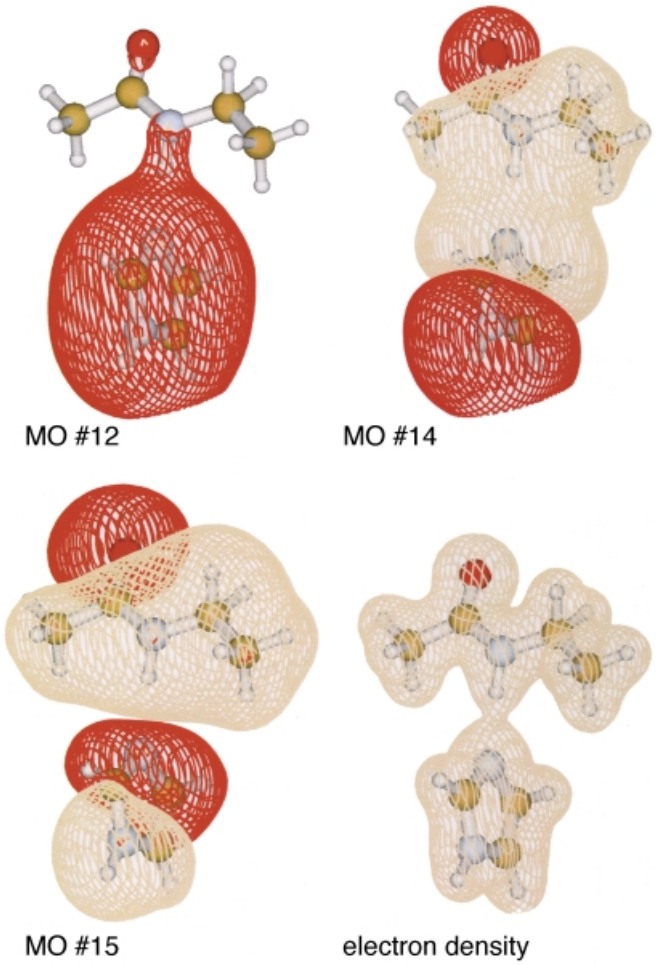

Fig. 5. *Graphical representation of three occupied molecular orbitals MO12, MO14, MO15 and the total electron density calculated for the initial molecular orientation of AEM and IM.*

installation of deMon NMR on a *Linux-PC* and a *Dec-Alpha* computers and Dr. *Olga Malkina* of the Faculty of Natural Sciences of Bratislave, Slovakia for the deMon version with the FC-MO analysis.

REFERENCES

[1] A. J. Dingley, S. Grzesiek, *J. Am. Chem. Soc.* **1998**, *120*, 8293.
[2] K. Pervushin, A. Ono, C. Fernández, T. Szyperski, M. Kainosho, K. Wüthrich, *Proc. Natl. Acad. Sci. U.S.A.* **1998**, *95*, 14147.
[3] K. Pervushin, C. Fernández, R. Riek, A. Ono, M. Kainosho, K. Wührich, *J. Biomol. NMR* **2000**, *16*, 39.
[4] G. A. Jeffrey, W. Saenger, 'Hydrogen Bonding in Biological Structures', Springer-Verlag, Berlin, 1991.
[5] K. Wüthrich, 'NMR of Proteins and Nucleic Acids', Wiley, New York, 1986.
[6] A. J. Dingley, F. Cordier, S. Grzesiek, *Concepts Mag. Res.* **2001**, *13*, 103.
[7] A. J. Dingley, J. E. Maase, R. D. Peterson, M. Barfield, J. Feignon, S. Grzesiek, *J. Am. Chem. Soc.* **1999**, *121*, 6019.

[8] A. Z. Liu, W. D. Hu, A. Majumdar, M. K. Rosen, D. J. Patel, *J. Biomol. NMR* **2000**, *17*, 79.
[9] A. Eletsky, T. Heinz, O. Moreira, A. Kienhöfer, D. Hilvert, K. Pervushin, *J. Am. Chem. Soc.* **2002**, submitted.
[10] M. Hennig, B. H. Geierstanger, *J. Am. Chem. Soc.* **1999**, *121*, 5123.
[11] I. G. Shenderovich, S. N. Smirnov, G. S. Denisov, V. A. Gindin, R. Reibke, S. Kirpekar, O. L. Malkina, H.-H. Limbach, *Ber. Bunsen-Ges. Phys. Chem.* **1998**, *102*, 422.
[12] H. Benedict, I. G. Shenderovich, O. L. Malkina, V. G. Malkin, G. S. Denisov, N. S. Golubev, H.-H. Limbach, *J. Am. Chem. Soc.* **2000**, *122*, 1979.
[13] E. D. Isaacs, A. Shukla, P. M. Platzman, D. R. Hamann, B. Barbiellini, C. A. Tulk, *Phys. Rev. Lett.* **1999**, *82*, 600.
[14] T. W. Martin, Z. S. Derewenda, *Nat. Struct. Biol.* **1999**, *6*, 403.
[15] T. Helgaker, M. Jaszunski, K. Ruud, *Chem. Rev.* **1999**, *99*, 293.
[16] A. Bagno, *Chem.–Eur. J.* **2000**, *6*, 2925.
[17] J. E. Del Bene, S. Perera, R. Bartlett, *J. Phys. Chem. A* **2001**, *105*, 930.
[18] W. F. van Gunsteren, S. R. Billeter, A. A. Eising, P. H. Hünenberger, P. Krüger, A. E. Mark, W. R. P. Scott, I. G. Tironi, 'Biomolecular Simulation: The GROMOS96 Manual and User Guide', VDF, Zürich, 1996.
[19] P. Guntert, K. Wüthrich, *Comp. Phys. Comm.* **2001**, *138*, 155.
[20] Y. M. Chook, J. V. Gray, H. M. Ke, W. N. Lipscomb, *J. Mol. Biol.* **1994**, *240*, 476.
[21] K. Pervushin, R. Riek, G. Wider, K. Wüthrich, *Proc. Natl. Acad. Sci. U.S.A.* **1997**, *94*, 12366.
[22] J. E. Ladner, P. Reddy, A. Davis, M. Tordova, A. J. Howard, G. L. Gilliland, *Acta Crystallogr., Sect. D: Biol. Crystallogr.* **2000**, *56*, 673.
[23] V. G. Malkin, O. L. Malkina, M. E. Casida, D. R. Salahub, *J. Am. Chem. Soc.* **1994**, *116*, 5898.
[24] V. G. Malkin, O. L. Malkina, L. A. Eriksson, D. R. Salahub, in 'Modern Density Functional Theory: A Tool for Chemistry, Vol. 2', Ed. J. M. Seminario, P. Politzer, Elsevier Science BV, Amsterdam, 1995, p. 273–347.
[25] H. Fukui, *Prog. Nuc. Mag. Res. Spec.* **1999**, *35*, 267.
[26] J. Kowalewski, A. Laaksonen, B. Roos, P. Siegbahn, *J. Chem. Phys.* **1979**, *71*, 2896.
[27] D. L. Beveridge, 'Semiempirical Methods of Electronic Structure Calculation', Plenum Press, New York, 1977, p. 163.
[28] A. St-Amant, D. R. Salahub, *Chem. Phys. Lett.* **1990**, *169*, 387.
[29] W. Kutzelnigg, U. Fleischer, M. Schindler, 'NMR Basic Principles and Progress', Springer, Berlin, 1990, p. 165.
[30] J. P. Perdew, W. Yue, *Phys. Rev. B* **1986**, *33*, 8800.
[31] M. J. Frisch, G. W. Trucks, H. B. Schlegel, G. E. Scuseria, M. A. Robb, J. R. Cheeseman, V. G. Zakrzewski, J. A. Montgomery Jr., R. E. Stratmann, J. C. Burant, S. Dapprich, J. M. Millam, A. D. Daniels, K. N. Kudin, M. C. Strain, O. Farkas, J. Tomasi, V. Barone, M. Cossi, R. Cammi, B. Mennucci, C. Pomelli, C. Adamo, S. Clifford, J. Ochterski, G. A. Petersson, P. Y. Ayala, Q. Cui, K. Morokuma, D. K. Malick, A. D. Rabuck, K. Raghavachari, J. B. Foresman, J. Cioslowski, J. V. Ortiz, A. G. Baboul, B. B. Stefanov, G. Liu, A. Liashenko, P. Piskorz, I. Komaromi, R. Gomperts, R. L. Martin, D. J. Fox, T. Keith, M. A. Al-Laham, C. Y. Peng, A. Nanayakkara, C. Gonzalez, M. Challacombe, P. M. W. Gill, B. G. Johnson, W. Chen, M. W. Wong, J. L. Andres, M. Head-Gordon, E. S. Replogle, J. A. Pople, Gaussian 98, Revision A.9, *Gaussian, Inc.*, Pittsburgh PA, 1998.
[32] G. Schaftenaar, J. H. Noordik, *J. Comput.-Aided Mol. Design* **2000**, *14*, 123.
[33] D. A. Case, C. Scheurer, R. Bruschweiler, *J. Am. Schem. Soc.* **2000**, *122*, 10390.
[34] G. Cornilescu, B. E. Ramirez, M. K. Frank, G. M. Clore, A. M. Gronenborn, A. Bax, *J. Am. Chem. Soc.* **1999**, *121*, 6275.
[35] A. C. Wang, A. Bax, *J. Magn. Reson.* **1997**, *127*, 54.
[36] J. P. Perdew, Y. Wang, *Phys. Rev. B* **1992**, *45*, 13244.
[37] S. Tsuzuki, H. P. Lüthi, *J. Chem. Phys.* **2001**, *114*, 3949.
[38] F. Jensen, 'Introduction to Computational Chemistry', John Wiley & Sons, Chichester, 1990, p. 172–173.

Received July 17, 2002